Proceedings of the Korean Nuclear Society Spring Meeting
Cheju, Korea, May 1996

Numerical Calibration method of an Electrochemical Probe for Measurement of Wall-Shear-Stress in Two-Phase Flow

Ki Yong Choi and Hee Cheon No
Korea Advanced Institute of Science and Technology

Abstract

The one-third calibrating relation by steady solution can cause large error when applied to an unsteady flow with large amplitude waves. Extended calibrating method, which can treat the normal convective contribution, is developed. The normal mass convective term is included into the 2-D mass transport equation by means of rms value and random function. The unknown shear rate is numerically determined by solving the 2-D mass transport equation inversely. This recovery method which predicts the unknown shear rate is constructed. It is found that it works very well without distortion. The inclusion of the normal convective term has a negligible effect on the mass transfer coefficient.

1. Introduction

The liquid-to-wall shear stress in stratified or annular two-phase flow, τ_{wL}, is usually evaluated by the Blasius-type friction factor. Andreussi and Persen(1987) reported that, at the onset of 2-D waves, f_L increases sharply, indicating an increase in turbulent dissipation in the liquid film. Miya et al.(1971) and Zabaras(1985) observed that a large increase in wall shear stress due to an increase in film thickness. Thus, the liquid-to-wall shear stress cannot be obtained by a Blasius-type correlation in two-phase flow system.

It is very difficult to measure the velocity gradient near a wall because the momentum boundary layer thickness is so thin. The mechanical instrumentation such as Stanton tube, Preston tube disturbs the flow field in such a thin boundary layer so that it is not a promising technique. Instead, a electrochemical instrumentation using a ferro-ferricyanide redox reaction at small cathodes embedded in the wall seems to be the most promising since it does not disturb a flow field near wall. This electrochemical probe is developed by Reiss and Hanratty(1962,1963). In principle, it can be calibrated analytically and not only the average value but also the local value of the mass transfer rate and/or shear stress at a liquid-wall interface can be measured. This method has been used extensively in various geometrical systems by many investigators: Mitchell et al.(1966), Sutey et al.(1969), Nakoyakov et al.(1981), and etc. However, it has disadvantage in that the frequency response is not so good. When a large amplitude fluctuation is imposed on the flow, the conventional steady calibrating relation cannot be used due to large distortion. Therefore, an extended calibrating method which can treat an unsteady flow such as wavy flow should be developed.

The mass transport equation governing the calibrating rule of the electrochemical probe has been solved neglecting the normal convective term. The normal convective term is of same order with the axial convective term grounded on the order of magnitude analysis. Therefore the effect of normal convective term should be also included into the extended calibrating relation.

2. Measuring Principle

An electrochemical reaction is carried out on the surface of an electrode mounted flush with the wall. A negative voltage applied to a test electrode drives a oxidation reaction of ferrocyanide at the cathode. The reverse reaction, i.e., reduction relation of ferricyanide, occurs at the counterpart anode electrode. The redox reaction occurring at two electrodes is as follows:

$$Fe(CN)_6^{3-} + e^- \longrightarrow Fe(CN)_6^{4-} \qquad \text{at the cathode}$$

$$Fe(CN)_6^{4-} \longrightarrow Fe(CN)_6^{3-} + e^- \qquad \text{at the anode}$$

As the applied potential is made higher, the current increases exponentially and thereafter approaches a constant value, i.e., a limiting current, asymptotically. This limiting current represents an operating condition under which the test electrode is in the process of concentration polarization. The total rate of mass transfer to the test electrode can be written

$$N = \frac{I}{n_e AF} = k_c C_b, \tag{1}$$

where N is the rate of mass transfer, I is the current, n_e is the number of electrons involved in stoichiometric reaction, A is a surface area of the cathode electrode, F is Faraday constant, k_c is a mass transfer coefficient, C_b is a bulk concentration.

A two-dimensional convective mass transport equation is written by

$$\frac{\partial C}{\partial t} + u\frac{\partial C}{\partial x} + v\frac{\partial C}{\partial y} = D(\frac{\partial^2 C}{\partial x^2} + \frac{\partial^2 C}{\partial y^2}), \tag{2}$$

where D is the diffusion coefficient of ferricyanide ions. Mass transfer between a turbulent fluid and a solid wall at high Schmidt number produces a very thin concentration boundary layer in the fluid. Levich(1962) obtained the relationship between a concentration and a momentum boundary layers as follows:

$$\frac{\delta_c}{\delta_v} \cong 0.6 Sc^{-1/3}, \tag{3}$$

where δ_c is a thickness of a concentration boundary layer and δ_v is a thickness of a momentum boundary layer. Since the thickness of the concentration boundary layer is very thin, the diffusion term in the streamwise direction can be neglected. The velocity components in the x and y direction are described by superposition of the wave-induced velocity fluctuation and the background turbulence. Thus, the instantaneous velocity is written by

$$u(x, y, t) = \overline{U}(x, y) + u'(t) + \tilde{u}(t), \tag{4}$$

$$v(x, y, t) = \overline{V}(x, y) + v'(t) + \tilde{v}(t), \tag{5}$$

where $\overline{U}$ and $\overline{V}$ represent the time-averaged velocities, u' and v' turbulent velocity fluctuations, and $\tilde{u}$ and $\tilde{v}$ wave-induced velocity fluctuations in x and y direction, respectively. It is assumed that the turbulent and wave-induced velocity fluctuations are statistically independent variables. The time-averaged values of the turbulent and wave-induced velocity fluctuations are zero.

The reported root-mean-square value of the streamwise velocity normalized with the friction velocity, u_{rms}/u^*, is linear with respect to y^+ and its magnitude shows scattering, which varies from 25% to 40% of the mean value. Since the rms level is not small enough to neglect, the contribution of the turbulence intensities to the instantaneous streamwise velocity cannot be neglected. Therefore, the fluctuating velocity due to the turbulence intensities can be approximated by by

$$u'(t) = u_{rms} F(t), \tag{6}$$

where $F(t)$ is normally distributed random variable with respect to time, of variance equal to unit and mean value of zero. When the flow is fully developed hydrodynamically and the measuring electrode is very small compared with the dimension of the channel, the x dependency of u can be neglected. Within so thin mass concentration boundary layer, the streamwise velocity is linear with y, so that the Eq.(4) can be written by

$$u(y, t) = [\overline{S} + \frac{u_{rms}}{\overline{U}} \cdot \overline{S} \cdot F(t) + \tilde{s}(t)] \cdot y \tag{7}$$

On the other hand, for the normal fluctuating velocity component, v', the rms level is suggested by several workers(Sirkar et al.(1970), Py (1973), Finnicum et al.(1985), Kim et al.(1987)). The

Table 1: Summary of the fluctuating velocity components

Author	Flow type	Measurement	$u_{rms}/(u^*y^+)$ or $u_{rms}/\overline{U}$	$v_{rms}/(u^*y^{+2})$
Mitchell et al.(1966)	pipe(water)	electrochemical	0.32	-
Sirkar et al.(1970)	pipe(water)	electrochemical	-	0.008
Reichardt (1971)	-	-	$0.24\exp(1/2\alpha y^+)$	-
Obermeier (1972)	-	-	$0.28 + C_1 y^{+2}$	-
Py (1973)	channel(water)	electrochemical	0.3	$2.43\frac{\nu}{\Lambda_{ux}}$
Eckelmann (1974)	channel(oil)	hot-film	0.24	-
Kreplin et al.(1979)	channel(oil)	hot-film	0.25	-
Finnicum et al.(1985)	pipe(water)	electrochemical	-	0.005
Kim et al.(1987)	numerical	-	0.37	0.009
Alfredsson et al.(1988)	channel	hot-wire		
	(oil, air, water)	hot-film	0.40	-

v_{rms}/u^* is quadratic function of y^+ close to a wall as summarized in Table 1. Since the $v'(t)$ distribution is much symmetric than the $u'(t)$ and closer to Gaussian(Kreplin et al.(1979)), $v'(t)$ is also represented by its root-mean-square value multiplied by random variable function. For a wave-induced fluctuation, $\tilde{v}(t)$, there is no available information. However, it is assumed that the waves at the gas-liquid interface do not penetrate into the liquid film deeply. The time-averaged normal velocity, $\overline{V}$, becomes zero for fully developed flow. Thus, the instantaneous normal velocity can be rewritten, neglecting the contribution of the wave-induced fluctuation as follows;

$$v(t) = v_{rms}F(t). \tag{8}$$

The independence between $u'(t)$ and $v'(t)$ is examined by comparing the correlation between them. In a very thin concentration layer, which the convective mass transport equation is applied to, the Reynolds shear stress, $-\rho\overline{u'v'}$, is very small close to a wall. It means that the fluctuating velocity components u' and v' are poorly correlated(Eckelmann et al.(1974) and Kim et al.(1987)). So, the u' can be treated independent of the v' in the vicinity of the wall.

3. Numerical Calibration

3.1 Direct Problem

Basically, the governing mass transport equation, which links the mass transfer rate with the wall shear stress, has a nonlinear convective term. Therefore, the relationship between the mass transfer rate and the wall shear stress can be obtained only by numerical calculation. In the same way as described by Mao and Hanratty(1991a, 1991b) the Eq.(2) can be written in a dimensionless form as

$$\frac{\partial C}{\partial \tau} + S(\tau)Y\frac{\partial C}{\partial X} + Sc^{2/3}L^{+1/3}v^+\frac{\partial C}{\partial Y} = \frac{\partial^2 C}{\partial Y^2}, \tag{9}$$

In the concentration boundary layer, the concentration changes dramatically at the leading edge of the electrode, and in the region close to the surface of the electrode. To minimize the effect of the leading edge, nonuniform grid sizes both in the x-direction and y-direction are used. The number of X-grid is selected 14 and Y-grid 50 because more larger grid value does not make any difference.

When the convective term is treated with an upwind scheme and the piecewise linear concentration profile is assumed, the following finite difference equation is obtained

$$A_p(i,j)C_{i,j}^{n+1} - A_u(i,j)C_{i,j+1}^{n+1} - A_d(i,j)C_{i,j-1}^{n+1} - A_l(i,j)C_{i-1,j}^{n+1} = C_{i,j}^n. \tag{10}$$

where

$$A_u(i,j) = \frac{\Delta\tau}{\delta Y_{j+1}\Delta Y_j} - \frac{\Delta\tau Sc^{2/3}L^{+1/3}v^{+n}}{\delta Y_j + \delta Y_{j+1}}, \qquad A_d(i,j) = \frac{\Delta\tau}{\delta Y_j \Delta Y_j} + \frac{\Delta\tau Sc^{2/3}L^{+1/3}v^{+n}}{\delta Y_j + \delta Y_{j+1}},$$

$$A_l(i,j) = S^n \Delta\tau Y_j/\delta X_i, \qquad A_p(i,j) = A_u(i,j) + A_d(i,j) + A_l(i,j) + 1$$

This finite difference equation can be expressed as a matrix form $AC^{n+1} = C^n$. The matrix, A, becomes a penta-diagonal matrix due to the diffusion term in the y-direction, of which components just above the diagonal term are zero. The initial concentration at each grid is set to 1, except of the surface of the electrode where the concentration is assigned a value of zero. For each time step, the concentration field is calculated by solving the above matrix with SOR method. Modified Sherwood number can be calculated by means of the following

$$Sh^* = \int_0^1 \frac{\partial C}{\partial Y}|_{Y=0} dX = \sum_{i=1}^{i_{max}-1} \frac{C(X_i, Y_1)}{\delta Y_1} \Delta X_i \tag{11}$$

3.2 Inverse problem

In the case of the direct problem, the mass transfer coefficient is obtained by solving the governing mass transport equation for a given shear rate. Whereas, in laboratory experiments, the mass transfer coefficient is given by measurement and the shear rate is unknown variable, implying that the governing equation should be solved inversely. It is impossible to analytically to obtain a past solution with a current solution due to the characteristic of the governing partial differential equation which has a diffusion term. So, the past shear rate has to be obtained numerically by an iterative method. It assumes the variation of the shear rate and the concentration profile at times $\tau \leq \tau_k$ are known. If the time step, $\Delta\tau_k$, is assumed to be very small, the modified Sherwood number at time τ_{k+1} can be written by

$$Sh_{k+1} \cong Sh_k + \frac{\partial Sh}{\partial S}|_{S_k}(S_{k+1} - S_k), \tag{12}$$

where $\frac{\partial Sh}{\partial S}|_{S_k}$ is a sensitivity coefficient at S_k, approximated by

$$\frac{\partial Sh}{\partial S}|_{S_k} \cong \frac{Sh[(1+\epsilon)S_k] - Sh[S_k]}{\epsilon S_k}, \tag{13}$$

where ϵ is a small perturbation factor. Therefore the shear rate s_{k+1} is obtained by substitution of the Eq.(13) into Eq.(12) and rearranging as the follows:

$$S_{k+1} \cong S_k + (Sh_{k+1} - Sh_k)\frac{\epsilon S_k}{Sh[(1+\epsilon)S_k] - Sh[S_k]}. \tag{14}$$

Here, the term $Sh[S_k]$ can be replaced with the measured value of Sh_k due to the first assumption, but $Sh[S_{k+1}]$ is obtained by solving the direct problem once for a given $(1+\epsilon)S_k$. As the formula defined in Eq.(14) is a kind of linear approximation, the calculated value of S_{k+1} is not a true value. Therefore S_{k+1} is adjusted until the calculated Sherwood number at τ_{k+1} is reasonably close to the measured Sh_{k+1}. This root-finding job is done by a simple algorithm called by bisection method.

4. Results and Discussions

To investigate the frequency response of the probe and the effect of the large amplitude variation of the shear stress, Eq.(9) is solved numerically by assuming a sinusoidal variation of the shear rate, that is,

$$S(n) = 1 + \hat{s}\sin(2\pi f n d\tau), \tag{15}$$

where $\hat{s}$ is the fluctuating amplitude of the shear rate and f is the frequency. In the present work, the fluctuating amplitude of the shear rate and the frequency are varied to study their effects on the mass transfer probe. Figure 1. shows the results. The calculated values are compared with the quasi-steady state solution. As the frequency increases, the modified Sherwood number no longer has the sinusoidal shape. Figure 2. shows the effect of the normal velocity on the modified Sherwood number. The four kinds of random sequences, which have the same statistical properties, are simulated. As can be seen in Figure 2, the effect of the normal velocity is minor.

To check whether the inverse method works well, the modified Sherwood number, which was already calculated by the direct problem solver, is used as an input for the inverse problem. The solution of the inverse problem should be reasonably close to the sinusoidal shear rate which was used in the direct problem. Figure 3 shows the results for the case of $f = 0.4$ and $\dot{S} = 0.9$. The input shear rate is predicted through the solution of the inverse problem with a surprising accuracy, implying that the numerical tool works very well. In this numerical simulation, the initial shear rate is assumed to unit and the corresponding concentration field is assumed to be a known value. So, a few points from the initial step show some difference from the reference value as can be seen in the figure 3. However, it seems that it does not affect the future calculation severely. After a few calculation, the solution has a tendency of approaching the reference value. The estimation of the shear rate was in good agreement with the reference shear rate. It is necessary to check whether the inverse method can deal with the complex signal having many frequency components with the same accuracy and stability. A total of 1,024 points are normalized with the average value to simulate the dimensionless shear rate. Then the modified Sherwood number is calculated through the direct method. Based on the calculated Sherwood number, the shear rate is again obtained by both the quasi-steady state solution and the inverse method with and without normal convective term. The result is shown in figure 4. As can be seen in figure 4, the inverse method reconstructs the original shear rate very well. For more detail comparison, the first part of the figure 4 is enlarged and shown in the figure 5. The prediction by the quasi-steady state solution is much smoothened due to the time delay of the signal, which means the loss of the information with high frequency. Whereas, the prediction by the inverse method shows a very good agreement with the reference value. It is thus concluded that the quasi-steady state solution is not applicable to the unsteady flow, but the inverse method can predict the real variation of the shear rate very well even in a complex situation. On the other hand, the inclusion of the normal convective term has a negligible effect on the mass transfer coefficient contrary to expectation. It is caused by the very thin mass concectration boundary layer. The thickness of the mass concentration boundary layer at the end of the electrode is calculated about $y^+ \cong 1$.

References

[1] Andreussi, P. and Persen, L.N. 1987 *Int. J. Multiphase Flow* **13** 565–575.
[2] Miya, M., Woodmansee, D.E. and Hanratty, T.J. 1971 *Chem. Eng. Sci.* **26** 1915–1931.
[3] Zabaras, G.J. 1985 *Ph.D. Thesis, Dept. of Chemical Eng., Univ. of Houston.*
[4] Reiss, L. P., Hanratty, T.J. 1962 *AIChE J.* **8**, 245–247.
[5] Reiss, L. P., Hanratty, T.J. 1963 *AIChE J.* **9**, 154–160.
[6] Mitchell, J. E., Hanratty, T.J. 1966 *J. Fluid Mech.* **26**, 199–221.
[7] Sutey, A. M., Knudsen, J.G. 1969 *AIChE J.* **15**, 719–726.
[8] Nakoyakov, V. E. et al. 1981 *Int. J. Multiphase Flow* **7** 63–81.
[9] Levich, V. G. 1962 Physicochemical hydrodynamics. 683–688.
[10] Sirkar, K. K., Hanratty, T.J. 1970 *J. Fluid Mech.* **44**, 589–603.
[11] Py, B. 1973 *Int. J. Heat Mass Transfer* **16**, 129–144.
[12] Finnicum, D.S. and Hanratty, T.J. 1985 *Phys. Fluids* **28**, 1654–1658.
[13] Kim, J., Moin, P. and Moser, R. 1987 *J. Fluid Mech.* **177**, 133–166.
[14] Kreplin, H.P. and Eckelmann, H. 1979 *Phys. Fluids* **22**, 1233–1239.
[15] Eckelmann, H. 1974 *J. Fluid Mech.* **65**, 439–459.
[16] Mao, Z. and Hanratty, T.J. 1991a *Int. J. Heat Mass Transfer* **34** 281–290.
[17] Mao, Z. and Hanratty, T.J. 1991b *Exp. in Fluid* **11** 65–73.

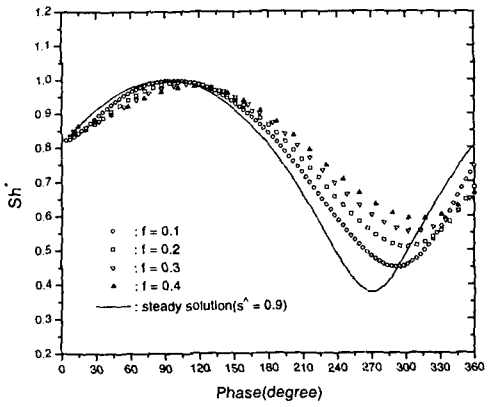

Figure 1. Frequency response of the modified Sherwood number

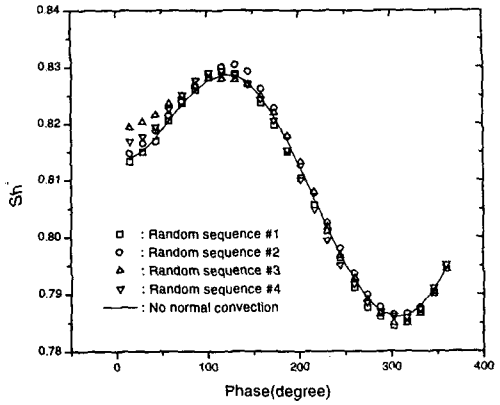

Figure 2. Contribution of the normal convective term on the modified Sherwood number (f=0.4, s^=0.1)

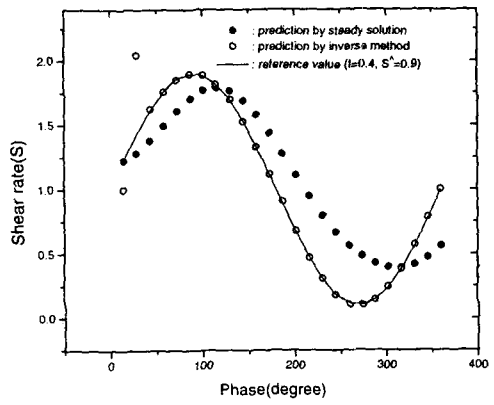

Figure 3. Shear rated predited by inverse method

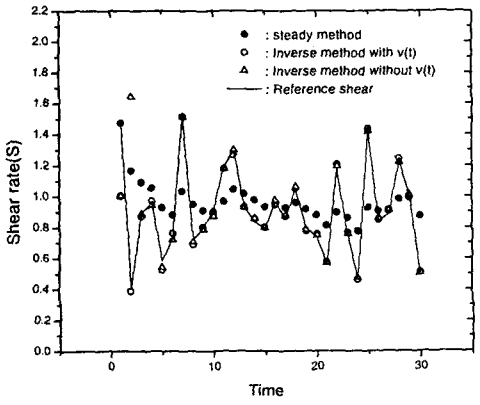

Figure 5. Enlarged diagram of the solution by the inverse method for an arbitrary signal

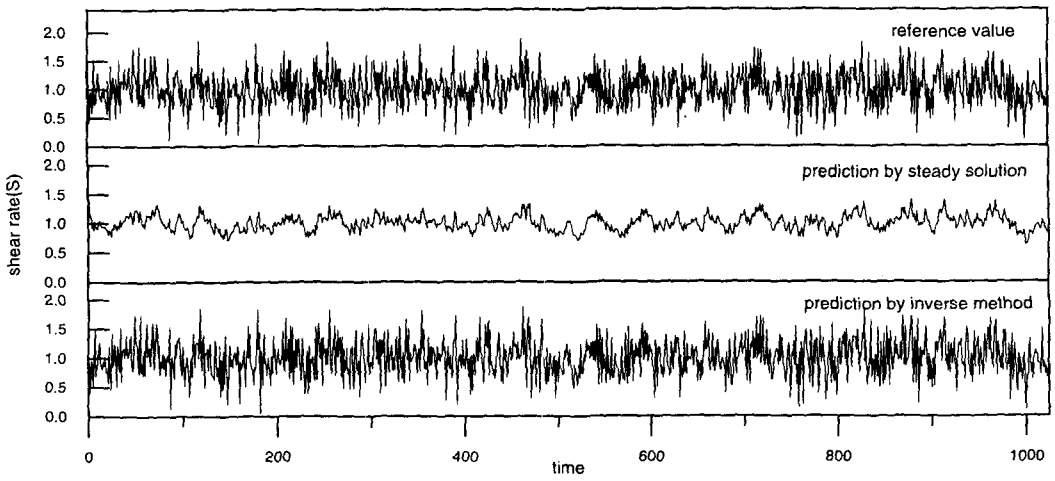

Figure 4. Prediction by inverse method for an arbitrary sigmal